TOWARDS THE SYNTHESIS OF SEGMENTED POLYTHIOPHENES

by

Ramzi Hader

B.Sc. , Simon Fraser University, 1991

A THESIS SUBMITTED IN PARTIAL FULFILLMENT
OF THE REQUIREMENTS FOR THE DEGREE OF
MASTER OF SCIENCE
in the Department
of
Chemistry

SIMON FRASER UNIVERSITY

March 1994

APPROVAL

Name: Ramzi Hader

Degree: Master of Science

Title of Thesis: Towards the Synthesis of Segmented Polythiophenes

Examining Committee:

Chair: Dr. F.W.B. Einstein

Dr. S. Holdcroft, (Assistant Professor)
Senior Supervisor

Dr. K.N. Slessor, (Professor)
Committee Member

Dr. L.K. Peterson, (Associate Professor)
Committee Member

Internal Examiner: Dr. T.N. Bell, (Professor)

Date Approved: March 10, 1994

PARTIAL COPYRIGHT LICENSE

I hereby grant to Simon Fraser University the right to lend my thesis, project or extended essay (the title of which is shown below) to users of the Simon Fraser University Library, and to make partial or single copies only for such users or in response to a request from the library of any other university, or other educational institution, on its own behalf or for one of its users. I further agree that permission for multiple copying of this work for scholarly purposes may be granted by me or the Dean of Graduate Studies. It is understood that copying or publication of this work for financial gain shall not be allowed without my written permission.

Title of Thesis/Project/Extended Essay:

Towards The Synthesis of Serrata

Author:

(signature)

(name)

(date)

Towards the Synthesis of Segmented Polythiophenes

Abstract

Novel segmented thiophene oligomers consisting of π-conjugated blocks separated by alkyl spacers were synthesized by copolymerization of 2,5-diiodothiophene with 1, 10-di((5-iodo)-2-thienyl)decane via the Grignard method. The materials possessed alternating rigid and flexible segments structure as confirmed by UV - vis, IR, and ^1H NMR spectroscopies.

The oligomers formed uniform free-standing films. A thermal polarization microscopy study of the films revealed the existence of a nematic liquid crystalline phase at temperatures above 70 ^oC.

The conductivity of oxidized films of these oligomers was 10^{-3} to 10^{-4} S / cm. This low conductivity is a direct consequence of restricted intramolecular conduction. These results provide insight into the contribution of the intermolecular conduction mechanism to charge transport in polythiophenes.

ACKNOWLEDGMENTS

" Al humdo wa a shukrou lee allahe rub al allameen wa a salato wa a salamo ala ashroughe al mursalleen, sydena Mohammeden wa ala aleehe wa cuhbehe ajmaaeen ".

Translation

" Praises and thanks to Allah, god of the worlds, and prayers and peace be upon the most honorable of messengers, Mohammed, and on his family and companions all."

I would like to thank Dr. Steve Holdcroft for his assistance and patience during the course of this project.

I would also like to extend my thanks to Dr. Keith Slessor for his helpful comments on my work.

I would like to express my appreciation to Dr. John Bechhoefer for allowing us to utilize his polarization microscopy equipments and to his student Anand Yethiraj for all his help.

I would also like to thank our lab group for their support, especially Isabel Arroyo and Mohammed Abdou for their helpful insights and discussions.

Finally, my thanks to all the university support staff that have contributed to the making of this thesis.

TABLE OF CONTENTS

LIST OF TABLES

PAGE

LIST OF FIGURES

PAGE

CHAPTER I INTRODUCTION:

To keep up with our ever developing technology, a continuous search for new materials with unique properties for use in new applications or to selectively improve existing ones has to be maintained. This vigilance led to the 1977 discovery that an intrinsically insulating organic polymer, polyacetylene, can be made highly conductive by exposing it to oxidizing or reducing agents[1]. The above procedure is referred to as a doping process. This finding opened the door to a new field and has led to the evaluation and development of various organic polymers which give a response similar to that of polyacetylene in its oxidized or reduced form. This effort has yielded a number of organic polymers with interesting electronic properties. Polymers such as polyparaphenylenes, polypyrroles, and polythiophenes are examples of this new class of polymers[2]. Figure 1 shows some of the more important conductive polymers known to date.

These polymers have the potential to combine the low density, processability, and resilience against corrosion of plastics with metallic properties. This combination makes them potentially useful in a wide range of applications extending from antistatic coatings to selectively modified electrodes and sensors[3]. However, poor characterization and a lack of understanding of their physicochemical and electrical properties have impeded their technological application.

Polythiophenes are considered one of the promising classes of conducting polymers for technological use. This is attributed to their good environmental stability in the neutral form[4], their structural versatility which allows their

Some of the important conductive polymers

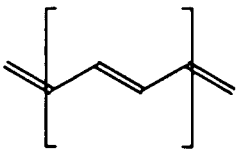

poly(acetylene)

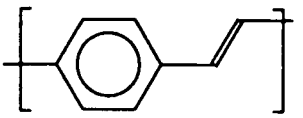

poly(paraphenylenevinylene)

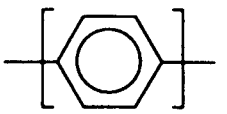

poly(paraphenylene)

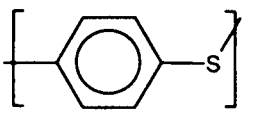

poly(paraphenyenesulfide)

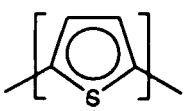

poly(thiophene)

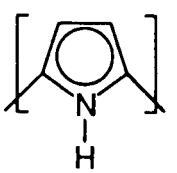

poly(pyrrole)

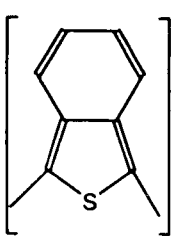

poly(isothianaphthene)

FIGURE 1

electronic and electrochemical properties to be modified by chemical means[3], and their intrinsic characteristic of having non degenerate ground states[5] for the two limiting structures of polythiophene shown in Figure 2.

The two main disadvantages of polythiophenes are their infusibility and their insolubility which result from strong interchain stacking and relative chain rigidity. In 1986, the problem was reduced significantly by the grafting of flexible hydrocarbon chains onto the conjugated polythiophene backbone. The substitution was achieved at the monomeric level at the 3-position of the thiophene ring[6,7,9]. The substituted thienyls were then polymerized by a number of chemical and electrochemical methods to yield poly(-3-alkylthiophenes)[6,7-17]. The flexible substituents solubilized the polythiophene chains by disrupting their interchain stacking[6,9,10]. This in turn facilitated the processability of these polymers[6,10,12]. Generally, the 3-alkyl thienyls couple via the 2- and 5-positions of the rings. However, the asymmetry of the substituted thiophenes gives rise to various regioisomers[10,16-22] which are shown in Figure 3. The synthetic method and conditions have become instrumental in determining the regiochemistry of the resulting polymers. The regiochemistry was found to have a profound effect on the optical and electronic properties[16-24], as well as on the morphology of a polymer. The effect is attributed to the steric strain imposed by having two or more of the alkyl side chains in close proximity. Naturally, the polymer attempts to alleviate the strain by partially rotating adjacent thienyl units, thus increasing the entropy of the chains as well as reducing their conjugation length[24].

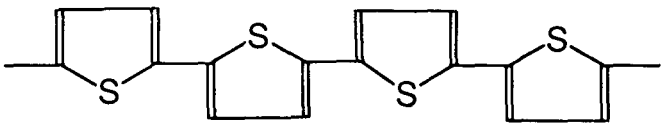

AROMATIC GROUND STATE

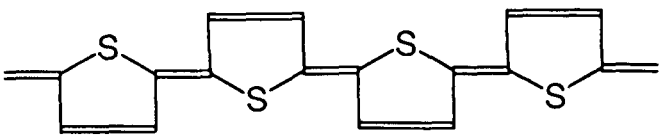

QUINOIDAL GROUND STATE

The ground state structures of polythiophene

FIGURE 2

It was found that different synthetic methods yields different percentages of the various regioisomers[24,25]. This versatility in synthetic methods has introduced problems in reproducibility and purity of the polymers. On the other hand, it provides methods of synthesizing application specific polymers. For instance, a head-to-tail linkage is desirable for a conductive polymer since it ensures coplanarity, high conjugation length as well as a high degree of crystallinity. While a head-to-head linkage is ideal for photoluminescence applications since it disrupts non-radiative decay processes such as intermolecular decay manifolds and in turn increases the efficiency of photo-emissive processes[26]. This is attributed to the decrease in coplanarity, crystallinity and conjugation length of the chains observed with head-to-head linkages.

It is appropriate at this point to review the origin of conductivity in polythiophenes. This will serve to introduce the project and describe the contribution of this work to the on going research in the area

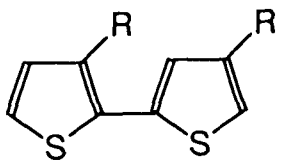

HEAD-TO-TAIL

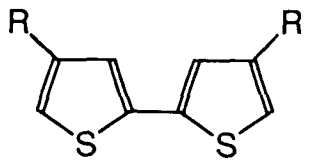

TAIL-TO-TAIL

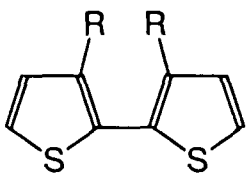

HEAD-TO-HEAD

Regioisomers of poly(3-alkylthiophene)

FIGURE 3

I.2 Charge transport in polythiophenes:

There are two modes of charge conduction in polymers. One is referred to as ionic charge conduction in which the charge carriers are ions. This mode does not apply to the polymers described in this study. The other mode of conduction is electronic charge conduction in which the charge carriers are electrons or positive holes depending on the polymer.

In polythiophenes and their derivatives, positive holes are considered to be the most prominent charge carriers in the conduction process[5]. This can be illustrated using band theory. As for organic molecules in general, the theory states that the highest occupied molecular orbitals, HOMO, interact to form the valence band, while all lowest unoccupied molecular orbitals, LUMO, interact to give the conduction band. For polythiophenes, the two bands are separated by an energy gap of approximately 2.2 eV which makes them semiconductors in the undoped state. When a polymer chain is doped, a hole is introduced in the valence band. This results in a structural rearrangement around the charge. The lattice relaxes into a quinoidal ground state and a polaron state is introduced into the energy gap. The change in local geometry favors the localization of charge in the region of rearrangement which in turn favors the loss of another electron to form a bipolaron. As the percentage doping increases, more bipolaronic states are formed. It was found that the formation of bipolaronic states is energetically favored over the formation of single polaronic states[27]. As the percentage doping is increased even further, the bipolaronic states overlap to form two new bands in the gap. Refer to Figure 4 for a visual representation of the process described above. It was found experimentally that the polymer showed this metallic character when doped at > 30 mole%[2d,5].

This theory however, fails to describe the mechanism of charge propagation through a polymer film. The consensus is that the conductivity of a film is the function of two processes:

- An intrachain mechanism, where the bipolaron is accelerated along one chain. This process is fast and it is dependent on the degree of coplanarity as well as on the conjugation length of the polythiophene backbone.

* An interchain mechanism, where the bipolaron hops from: (a) one chain on to another; (b) one segment of a chain on to another; or (c) one cluster of chains on to another. This process is slow and is dependent on the degree of crystallinity of the polymer. This mechanism is suspected of being the bottleneck in the process of charge propagation.

Very little work has been done in this area[28-31]. However, it was found that the conductivity of polythiophene films is highly anisotropic. Polymer films have conductivities which are in the order of 0.6 S/cm when measured parallel to the surface of the film and 1.0x 10^{-4} S/cm when measured perpendicular to the surface of the film[28]. It is of interest to polymer scientists, if the contributions of the two charge propagation mechanisms were isolated and possibly quantified.

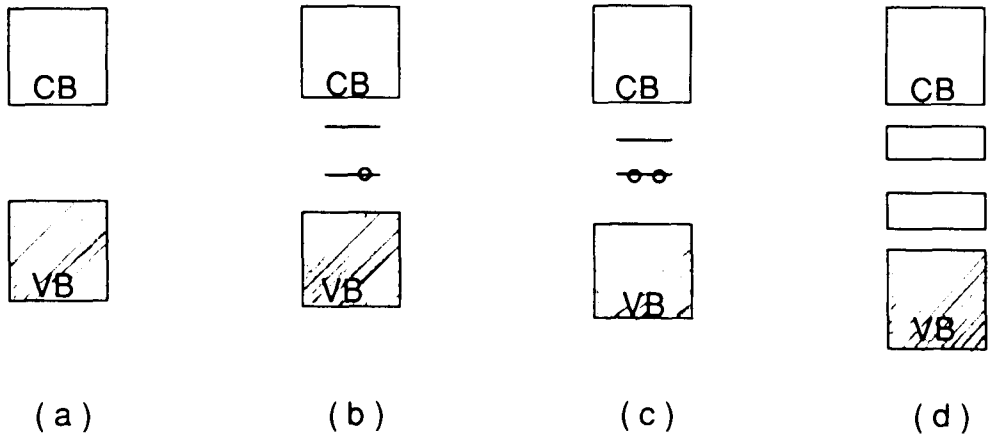

(a) undoped, (b) formation of a polaron, (c) formation of a bipolaron, (d) 30 mole % doping bipolaron states overlap to form two bands.

FIGURE 4

Considering the facts mentioned above, it is desirable to obtain a polymer which is soluble, has indistinguishable linkages and one of the two charge transport mechanisms isolated. A solution to the dilemma is to synthesize a polymer that has rigid conductive segments of three to six thiophene rings linked by flexible non conductive alkyl chains. The alkyl chains serve to solublize the polymer and disrupt the intrachain charge conduction mechanism. This design also eliminates the problem of regioisomerism observed with poly(3-alkyl thiophenes) and should enhance the crystallinity of the polymer and thus help isolate the interchain mechanism contribution to the conduction process. In the following sections, the synthesis and characterization of this novel class of conducting polymers are reported.

CHAPTER II SYNTHESIS:

Chemical and electrochemical methods are the most popular routes for synthesizing poly(-3-alkylthiophenes)[6-17]. Electrochemically, poly(-3-alkylthiophenes) with alkyl chains containing 1 to 20 carbons have been prepared[10,32-34]. Using the chemical route, polymers have been synthesized by oxidative coupling of the substituted thienyls by Lewis acids such as $FeCl_3$[11-13] or by nickel catalyzed Grignard coupling of the 2,5-dihalothiophene monomers[16,17,19,36-41]. For this project, the synthetic approach is to prepare two reactive monomers which can be copolymerized to yield the target polymer. The monomers chosen were 2,5-diiodothiophene (C) and 1,10-di((5-iodo)-2-thienyl)decane (B). The monomers were polymerized via the Grignard method with the use of 1,3-bis(diphenylphosphino)propane nickel(II) chloride as catalyst. Figure 5 shows the chemical formulae of the chemical substances described in the detailed synthetic procedure.

II.2 CHEMICALS AND INSTRUMENTATION:

All chemicals named were used as received. Thiophene, 1,10-diiododecane, and 2.5 M n-butyllithium were obtained from Aldrich chemicals. Iodine and mercuric oxide were purchased from BDH chemicals. Solvents were dried by refluxing over sodium metal wire under a flow of nitrogen gas. Gas chromatographic analysis was performed on a Hewlett-Packared 5890 chromatograph. Electron impact (70eV) mass spectra were obtained with a Hewlett-Packard 5985 GC.MS instrument. IR spectra were recorded on a Bomem Michelson FTIR (120 series). UV-vis spectra were recorded on a Hewlett-Packard 8452A spectrophotometer. ^1H NMR spectra were obtained

using a Bruker AMX 400 (400MHz) NMR spectrometer. Gel permeation chromatography data was determined using 10^5, 10^4, and 10^3 A° μ styrogel columns at 25 °C. Oligomers were eluted with tetrahydrofuran (BDH-HPLC grade) and detected using a UV-vis spectrophotometer from Waters (model 486). Differential scanning calorimetry analysis was performed on a Perkin Elmer differential scanning calorimeter-DSC7. Polarization microscopy study utilized an Olympus BH2-UMA polarizing microscope equipped with an INSTEC HS1-i hot stage.

II.3 SYNTHESIS OF 1,10-di(2-thienyl)decane (A):

99 mL of 2.5 M (0.25 moles) n-butyl lithium solution in hexanes were cooled under N_2 below 0 °C using an ice/NaCl cold bath. The solution was diluted with 130 mL of dry tetrahydrofuran and 40 mL of dry hexanes. The mixture was allowed to equilibrate in temperature for 15 minutes. 25 g (0.30 moles) of thiophene were added to the stirring reactants over a period of 15 minutes. A temperature increase was observed, but, the bath was cold enough to maintain the temperature below 0 °C. The cold bath was removed when the addition was complete. 50 g (0.13 moles) of 1,10-diiododecane were charged into the reaction vessel under a positive flow of nitrogen. The mixture was allowed to stir in the dark for two hours to avoid any decomposition that might occur due to the light sensitivity of 1,10-diiododecane. The heat released in the reaction can raise the temperature above the boiling point of hexanes, hence, a small condenser was used. After a gas chromatographic test, the excess n-butyl lithium was destroyed by the cautious addition of 200 mL of ice cold water to the vigorously stirring reactants. The organic and aqueous layers were allowed to separate in a separatory funnel. The aqueous layer was washed twice with 150 mL portions of

diethyl ether and the organic layers were combined and dried over magnesium sulphate. The solvents were rotoevaporated and the remaining yellow liquid was run through a 20 cm silica gel (240-400 mesh) column using a mixture of 10 : 1 hexanes : diethyl ether as an eluant. The eluant was removed and the product was vacuum dried. The yield was found to be 60 % and the results of the characterization were: U.V (THF): 248 nm (strong, broad). ^{1}HNMR ($CDCl_3$): 1.35 (m ,12H), 1.75 (p ,4H, β CH_2), 2.87 (t ,4H, α CH_2), 6.85 (2H, dd, $j_{3,4}$ 4.0 Hz, $j_{3,5}$ 1.2 Hz, H_3), 6.98 (2H, dd, $j_{4,5}$ 5.4 Hz, $j_{4,3}$ 4.0 Hz, H_4), 7.15 (2H, dd, $j_{5,4}$ 5.4 Hz, $j_{5,3}$ 1.2 Hz, H_5). G. C. - M. S. → *m/e* ($M^{+\bullet}$; 306). IR ($CHCl_3$, ν (cm^{-1}): 3009 m, 2930 s, 2857 s, 1464 m, 1433 m, 851 m, 820 m, 790 m.

II.4 SYNTHESIS OF 1,10-di((5-iodo)-2-thienyl)decane (B):

In a 1 L Erlenmeyer flask, 42 g (0.17 moles) of iodine were mixed with 24 g (0.11 moles) of mercuric oxide suspended in 30 mL of benzene. 17 g (0.06 moles) of monomer (A) were added dropwise while maintaining constant stirring. During the addition, the solution may become too viscous for stirring. In such a case, swirling the flask is recommended. The reaction was complete within four hours as determined by GC. The product was extracted using several washes with hexanes. The organic washings were combined and were washed with a solution of sodium thiosulphate in water to remove any unreacted iodine. The hexanes layer was dried over magnesium sulphate. After removal of solvent, the crude product was dissolved in a 50 : 50 mixture of diethyl ether and methanol from which it was crystallized out by slow addition of methanol. White flaky crystals were obtained in a 55% yield. MPR 40 - 45 °C. U.V (THF): 254 nm (strong, broad). ^{1}HNMR ($CDCl_3$) 1.30 (m,12H), 1.60 (p,4H, β CH_2), 2.79 (t,4H,

α CH_2), 6.46 (2H, d, $j_{3,4}$ 3.4 Hz, H_3), 7.03 (2H, d, $j_{4,3}$ H_4).G. C - M. S. → *m/e* ($M^{+\bullet}$; 558). IR ($CHCl_3$; ν (cm^{-1}): 3019 m, 2932 s, 2857 s, 1466 m, 1435 m, 939 m.

II.5 SYNTHESIS OF 2,5-diiodothiophene (C):

Using a setup similar to the one described in the synthesis of (B), 272 g (1.10 moles) of iodine were mixed with 155 g (0.72 moles) of mercuric oxide in 50 ml of benzene. 30 g (0.36 moles) of thiophene were slowly added to the stirred reactants[17]. The product was purified using the procedure utilized in the synthesis of monomer A. The product was obtained in 70% yield . U.V (THF): 248 nm (strong, broad), 294 nm (strong). ^{1}HNMR ($CDCl_3$) : 6.95 (1H, s, H_3 & H_4).

II.6 COPOLYMERIZATION OF (B) AND (C):

The magnesium di-Grignard reagent of monomer (C) in dry diethyl ether was formed by the slow addition of ether diluted monomer to a 2.2 molar excess of iodine-activated magnesium metal shavings. The reagent was allowed to reflux under nitrogen for two hours. From a dropping funnel, monomer (B) in diethyl ether was added dropwise. The mixture was allowed to stir for 1/2 hr. 1% by weight of monomer (C) of 1,3-bis(diphenylphosphino)propane nickel(II)chloride[16] was added under a positive flow of nitrogen along with dry diethyl ether in order to catalyze the coupling. The polymerization was allowed to proceed at a reflux temperature of ~ 40 °C for 24 hours. After the reaction had terminated, excess unreacted Grignard reagent was quenched by the cautious addition of methanol. The resulting polymer was precipitated from an excess of acidified methanol.

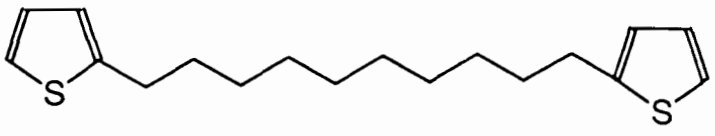

(A)

1, 10 - di(2 - thienyl)decane

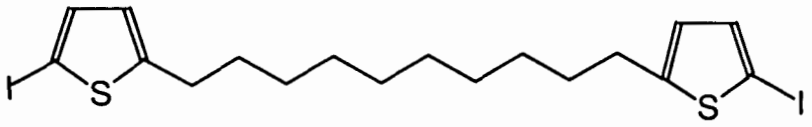

(B)

1, 10 - di((5 - iodo) - 2 - thienyl)decane

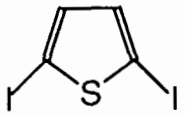

(C)

2, 5 - diiodothiophene

Chemical formulae of monomers

FIGURE 5

The product was collected and reprecipitated in the same manner from a solution of chloroform. Other methods of polymerization such as oxidative addition and formation of the di-Grignard of monomer (B) followed by coupling to monomer (C) were attempted, however, the method reported above was the most successful. It was observed experimentally that the formation of the di-

Grignard reagent of monomer (B) was considerably less favored than that of monomer (C). As far as the ratio of monomer (B) to monomer (C) in the polymerization reaction is concerned, the best results were obtained by using a 20 : 80 molar ratio of monomer (B) : monomer (C) which resulted in oligomers with 40 % yield. When the ratio of monomer (B): monomer (C) was increased the yields of the reactions decreased. For an equimolar ratio of the monomers virtually no oligomers were recovered. This led to the conclusion that monomer (B) has limited reactivity toward nucleophilic attack due to the increased electron density at the 2-position of the thienyl. It was also found that homopolymerization occurs during the formation of the di-Grignard reagent of monomer (C), yielding insoluble polythiophene if allowed to proceed. Furthermore, the homo-oligomers which form, coat the magnesium metal surface, thus terminating the reaction. In order to overcome the problems described above, monomer (B) was added when the formation of the Grignard of monomer (C) was ~ 40% complete. At this point, the majority of the reactive species in solution consisted of the mono-Grignard reagent. The restricting synthetic factors served to limit the length and yields of the targeted polymers. However, oligomers with interesting properties were obtained. In addition, the synthesis gave valuable insights pertaining to the modification of the starting monomers in order to improve the size, yield, and properties of products. Table 1 shows the different compositions of oligomers prepared.

TABLE 1 :Reactant Ratios and Product Yields

oligomers synthesized	% monomer (B)[a]	% decane spacer in oligomer[b]	% yield[c]
O1	20	18	45
O2	25	25	40
O3	40	40	30
O4	50	50	20

a= % monomer in reactants.

b= as determined from ^{1}H NMR.

c= calculated based on monomer (B).

CHAPTER III CHARACTERIZATION STUDIES:

III.1 Solubility:

Polythiophene is insoluble and infusible[2d]. Therefore, the solubility of the oligomers can provide insights on the nature of the product isolated. The oligomers were soluble in tetrahydrofuran, benzene, and chlorinated solvents such as chloroform and dichloromethane. Oligomers were generally less soluble than the better known poly(3-hexylthiophene), e. g., the solubility of oligomer(**O2**) in chloroform was 10 g/l in contrast to 30 g/l for poly(3-hexylthiophene). The lower solubility is explained on the basis that the decane spacers prevent aggregation of thienyl segments to a lesser degree than substituents grafted onto the main chain. The lower solubility of the oligomers also indicate a higher intermolecular order in the chain.

III.2 Ultraviolet - Visible Spectroscopy:

III.2.1 Introduction:

Solution UV - vis spectra of substituted polythiophenes show two main absorbance bands[41,42]. The low energy broad absorbance is assigned to a $\pi \rightarrow \pi^*$ transition of the entire chromophore, which is defined as the conjugated segment in the main chain. This transition is observed at wavelengths between 300 - 600 nm. The position of the wavelength maximum as well as the intrinsic color of the material were found to be directly dependent on the conjugation length of the thienyls in the main chain. The higher energy, narrower absorbance band (~ 250 nm) is associated with the local excitation of the sulfur atom in the individual thiophene ring and is not affected by the conjugation length of the macromolecule[43]. This transition is dependent only on the chemical structure of the ring and thus is characteristic of the presence of a thiophene ring. The UV - vis spectra of the oligomers provided information on the length of conjugation segments and on the optical effect of increasing the number of spacers within the oligomer molecule.

III.2.2 Results and discussion:

All the oligomers exhibited a broad absorbance band with three or more narrow peaks. The spectra are shown in Figure 6. The absorbance maxima along with their extinction coefficients are summarized in Table 2

Upon inspection of the data, a blue shift in the lower energy band maximum is detected as the molar ratio of decane spacer : thienyl is increased in the oligomer molecule. The shift is accompanied by a decrease in the extinction

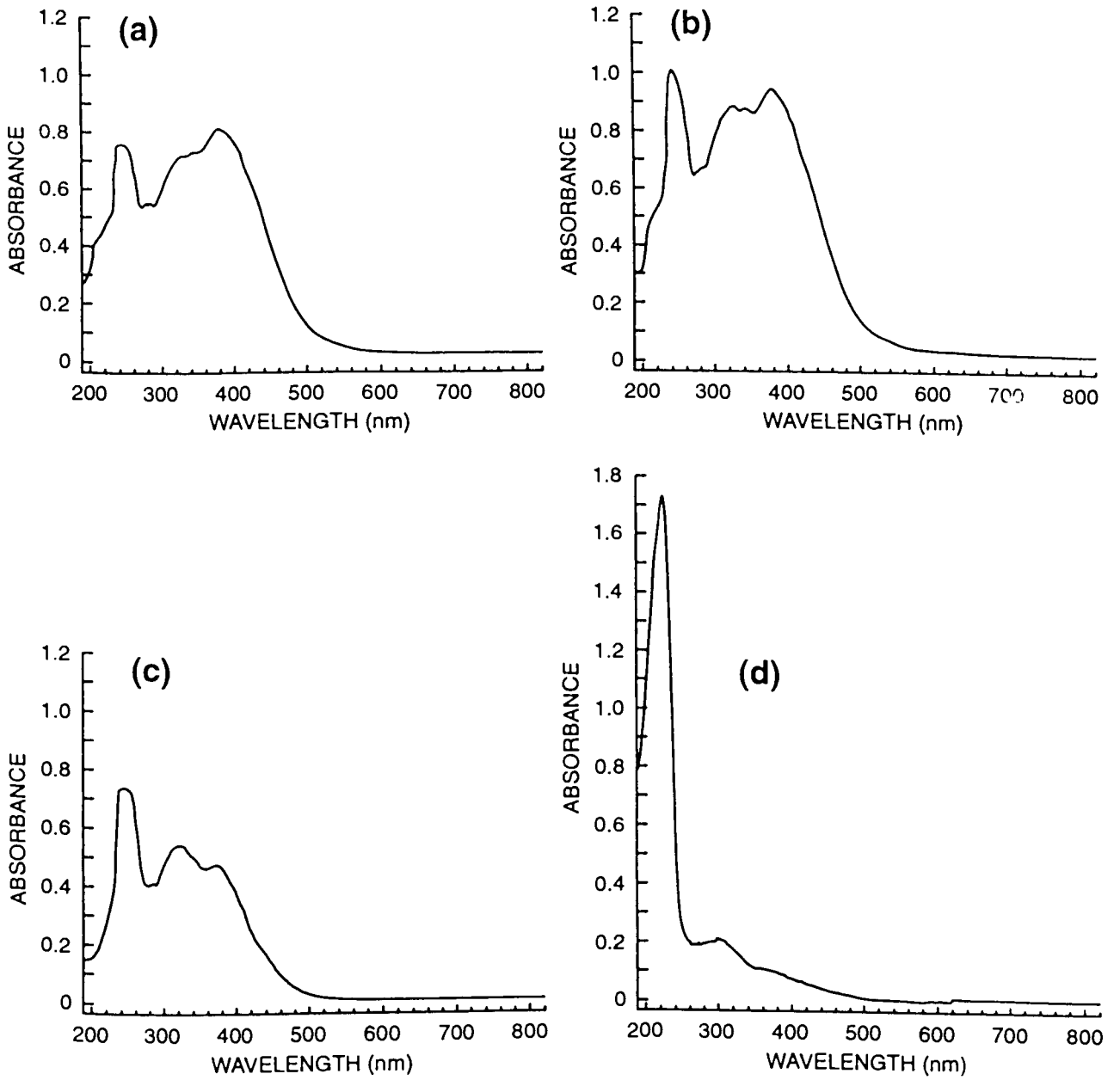

UV-vis spectra of: (a) oligomer (**O1**); (b) oligomer (**O2**); (c) oligomer (**O3**); and (d) oligomer (**O4**) in THF

FIGURE 6

TABLE 2 : UV - vis absorption data for various oligomers in THF

oligomer	conc^{n} (10^{-5}M)[b]	λ_1[c] (nm)	ε_1[d] (10^3 M^{-1} cm^{-1})	λ_2[c] (nm)	ε_2[d] (10^3 M^{-1} cm^{-1})	λ_3[c] (nm)	ε_3[d] (10^3 M^{-1} cm^{-1})
O1	7.05	380	11.5	324	9.93	246	10.6
O2	8.10	378	12.6	324	11.6	244	13.3
O3	11.0	372	4.27	324	4.82	244	6.64
O4	7.24	365	2.07	320	2.97	245	21.0
O2[a]	----	375	----	324	----	246	----

a = thin film spin-cast from chloroform solution.

b = concentration calculated using relative number average molecular weight obtained from GPC data.

c = wavelength of maximum absorption (nm).

d = extinction coefficients.

coefficient of the transition and is attributed to a shorter conjugation length. On the other hand, the sulfur atom local excitation transition maintained a wavelength which was independent of the number of decane spacers in the main chain. The oligomer absorbance maxima (λ_1,λ_2) reported in Table 2, provides qualitative information on the number of thienyls per conjugated segment averaged over the entire oligomer molecule rather than a representative average number of rings per segment. For instance, when λ_1 values are compared to the corresponding absorption band of terthiophene and quaterthiophene shown[41] in Table 3, the average number of thienyl per segment is determined to be between three to four rings. However, as a consequence of the synthetic method, the

actual number of rings per segment can vary between two to eight rings. Evidence for this is the extensive broadening of the lower energy absorption band which extends over a range of 300 nm and an absorbance tail that extends over 800 nm.

TABLE 3: UV - vis absorption data for oligomeric 2,5 thienylenes

Compound	λ_1 (nm) ($CHCl_3$)	λ_2 (nm) ($CHCl_3$)	ε_1 (10^3 M^{-1} cm^{-1})	ε_2 (10^3 M^{-1} cm^{-1})
Terthiophene	355	245	25.0	12.6
Quater-thiophene	390	248	45.5	20.5

The UV data cannot be used to determine the actual average number of rings per conjugated segment. However, the data is quite valuable in characterizing the effect of increasing the content of the non-conjugated segment (decane) on the effective conjugation length of the oligomer. As the ratio of decane spacer to thienyl increases, the effective conjugation length of the molecule decreases. This disables the intrachain conduction mechanism along the chain, in accordance with one of the project goals. The spectrum for oligomer (**O2**) in the solid state was found to be similar to that of the solution except for increased broadening of all the absorbance bands.(see Figure 7). The similarity of the two spectra leads to the conclusion that the effective conjugation length of the oligomer in solution and in solid state is similar which deviates from the observed for poly(3-hexylthiophenes). This implies that the oligomer molecule assumes a similar conformation in solid state and in solution. In other word, the oligomers are highly ordered in solutions.

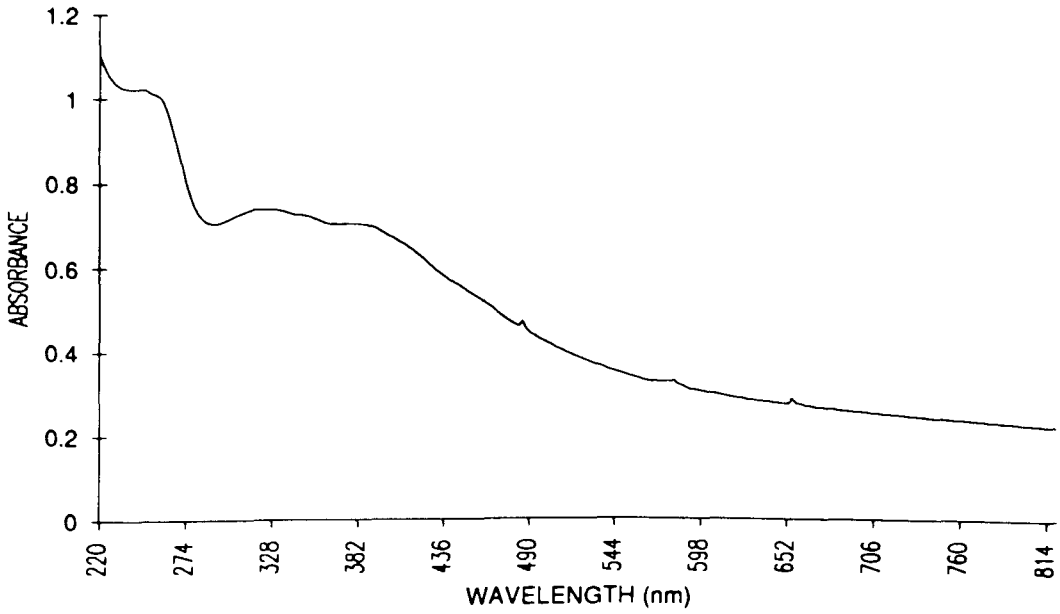

UV-vis absorption spectrum of oligomer (**O2**) thin film.

FIGURE 7

III.3 Proton Nuclear Magnetic Resonance:

III.3.1 Introduction:

NMR spectroscopy is one of the most powerful tools for obtaining structural information pertaining to an organic molecule. It is particularly useful in determining the local structures and conformations present in a polymer chain and how it relates to other chains in its vicinity. ^1H NMR spectra of polymers usually display complex splitting patterns over a small chemical shift range, and extensive line broadening. The latter is due to the large size of polymer molecules which causes them to tumble slowly in solution, and results in long spin relaxation times[44,45]. In a polymerization reaction, monomers can interlink through different binding sites which renders their protons chemically similar yet magnetically different. This results in further proton coupling which gives rise to the second order complex splitting patterns. Nevertheless, ^1H NMR is valuable in determining the types of linkage present, their percent occurrence in a polymer sample[44], and in confirming the identity of the monomers chemically bonded in the chain. Recently, 2D NMR was used in assignment of these complex multiplets by experiments such as COSY and NOESY[45].

III.3.2 Results and Discussion:

The ^1H NMR spectra of the oligomers, as represented by the spectrum of oligomer(**O2**) in Figure 8 , were run in deuterated chloroform. They possessed the following features:

- A broad singlet at 1.25 ppm due to six methylene hydrogens in the center of the alkyl chain spacer.
- A broad ill-defined multiplet at 1.65 ppm due to two methylene hydrogens

one carbon removed from the thienyls.

- A broad multiplet at 2.75 ppm due to two methylene hydrogens associated with the methylenes attached directly to the thiophene rings.
- A cluster of complex pattern peaks from 6.40 - 7.40 ppm due to the ring protons.

The assignment of the aromatic protons peak cluster is difficult due to the presence of varying lengths of thienyl segments and due to the presence of both proton terminated oligomers and iodine terminated oligomers. The majority of the thienyls are interlinked via the 2 and 5 position of the thiophene ring . However, the small possibility of a linkage through the 2 and 4 positions exists which complicates the assignment. This conventional ^1H NMR is ineffective for determining the average length of the thiophene segment in the molecule. However, the integration of the signal due to the aromatic protons peak cluster and that of the decane spacers proved useful in determining the ratio of decane spacers to thiophene rings in the oligomer molecule. Half the integral of the CH_2 multiplets at 2.75 ppm divided by the integral of the aromatic proton peak cluster yielded the average decane spacer to thiophene ratio in the oligomer chain which corresponded to the synthetically projected ratios presented in Table 1.

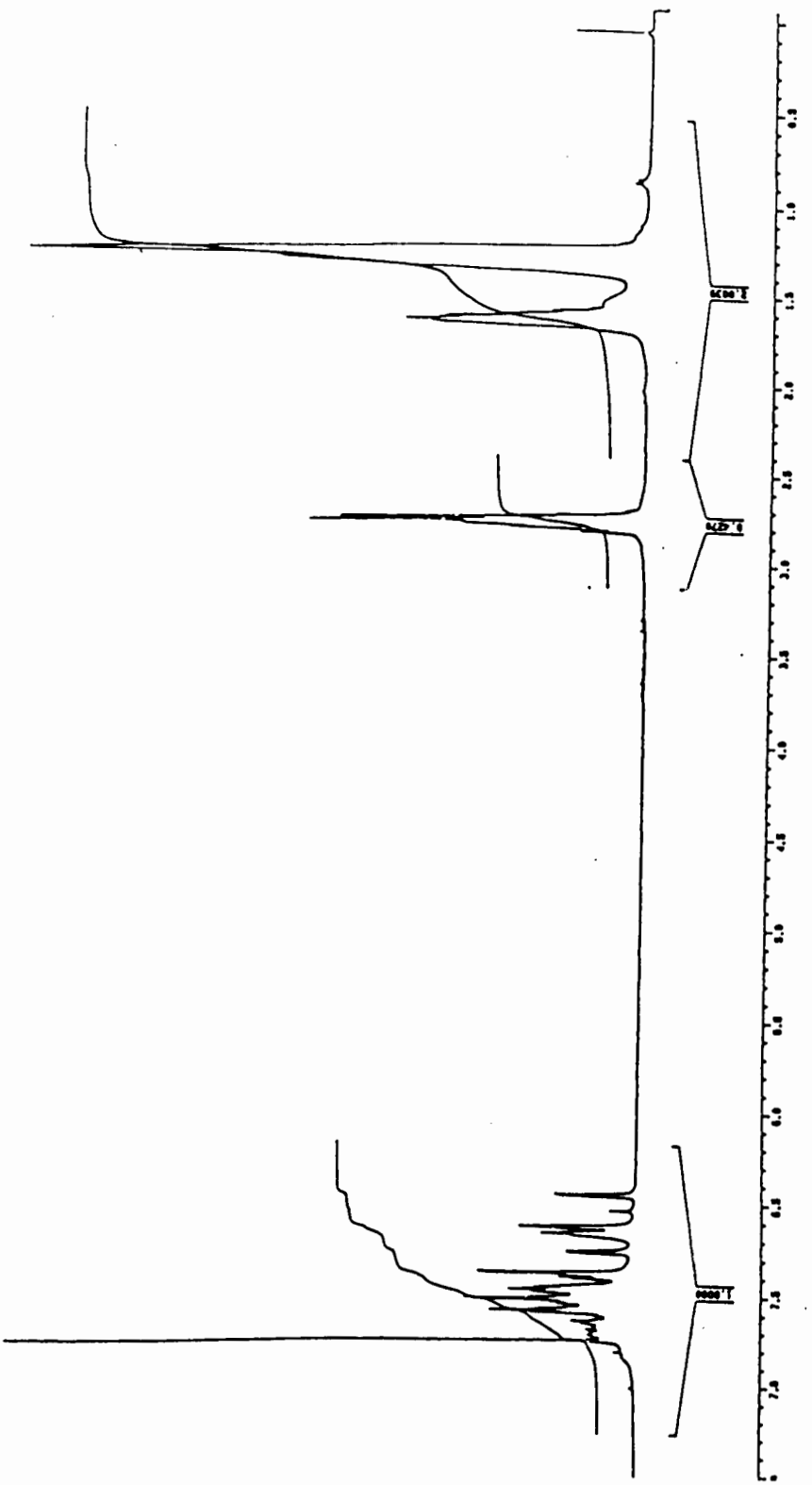

NMR spectrum of oligomer (**O2**) in $CDCl_3$

FIGURE 8

III.4 Gel Permeation Chromatography:

III.4.1 Introduction:

Gel permeation chromatography (GPC) is a technique for the separation of macromolecules according to their size. The process is summarized as follows. A diluted solution containing a broad molecular weight distribution of a polymer is forced under pressure through a column that is packed with finely divided solid particles. Each particle possesses pores (tunnels) of a particular diameter. As the solute passes each particle, the molecules with dimensions smaller than the diameter of the openings enter the pores and are delayed within the cavity. Molecules that are of the same size as the pore will be delayed to a lesser degree since they can not penetrate deep into the opening. The molecules with a random coil diameter larger than the pore's diameter are swept through by the solvent. This results in a separation in which larger molecules are eluted first, followed by medium sized molecules. Smallest molecules are eluted last. An effective separation can be achieved by linking a number of columns of different pore size in series. The columns are packed by either porous glass beads which are solvent independent or by a matrix of cross linked polystyrene which swells in a good solvent and generates the desired porosity[46,47]. There are two alternative methods of detection utilized in GPC. One method involves monitoring the change in the refractive index between the eluted solution and the pure solvent. A plot of the change in refractive index as a function of time can yield directly a plot of the molecular weight distribution. The accuracy of the procedure will be subject to the refractive index difference between the polymer and solvent. The response is dependent only on concentration and not on the molecular weight. The other method is UV detection, where an on-line spectrophotometer is set at an absorbance maximum of the polymer and the

absorbance is monitored as a function of elution time[46,47]. The GPC process is plagued with practical and data interpretation problems. Practical problems include the need to use small dilute samples in order to prevent the saturation of the pores; the possibility that a polymer chemically adsorbs on to polar substrates such a porous glass; and a change in the pores size of the cross linked polystyrene matrix in different solvents. These problems can be overcome by using one solvent system throughout the operation life time of the column, and by using low sample concentration such as 1 mg/ml. Interpretation of GPC data can be complicated by two important factors. First, the ease with which a polymer penetrates a pore will depend largely on whether it assumes a random coil or a rigid rod in the solvent system used. Thus, the polymer could have different chromatographic behavior in different solvents which could result in a false estimate of the molecular weight of the polymer. Second, the equipment has to be calibrated with monodispersed fractions of a different polymer (usually polystyrene) that has a similar conformation in solution, in order to correlate elution time with molecular weight. It is assumed that the calibration applies to the polymer of interest. However, the assumption does not hold at all times since different polymers can occupy different hydrodynamic volumes within the same solvent[47].

III.4.2 Results and Discussion:

Tetrahydrofuran was the solvent chosen to run the GPC since it is a good solvent for both the polystyrene matrix stationary phase and the oligomers synthesized. Table 4 shows the GPC data obtained.

The UV detector was set at the low energy $\pi \rightarrow \pi^*$ absorption maximum for each of the oligomers. The resulting spectra displayed one broad peak with

three narrower maxima which were used to calculate the number average and the weight average molecular weights. Figure 9 shows the GPC of oligomer (**O2**).

TABLE 4: Results of GPC measurements on the oligomers

Oligomer	M_n[a]	M_w[b]	MWD[c]
O1	1000	1650	1.6
O2	1200	1500	1.2
O3	1600	2400	1.5
O4	800	1100	1.4

a= number average molecular weight

b= weight average molecular weight

c= molecular weight distribution, polydispersity, (M_w/M_n)

The data in Table 4, can only be used as a relative measure of the molecular weight of the oligomers synthesized. This is a result of the fact that the GPC used was calibrated for poly(-3-hexylthiophene). The oligomers are less soluble than poly(-3-hexylthiophene), therefore, it is possible that they take on a different hydrodynamic volume, as well as, assume a different conformation in solution which in combination with the unavailability of the appropriate Mark - Houwink constants render the molecular weight values qualitative at best. However, the data can be used to gauge the effect of varying the ratio of the two monomers on the length of the resulting oligomers. It is apparent from the data in Table 4 that the molecular weight of the oligomers are within the same order of magnitude. The low reactivity of the 2 position of the thienyl in monomer (B) towards nucleophilic attacks may explain the observed limitation of chain growth.

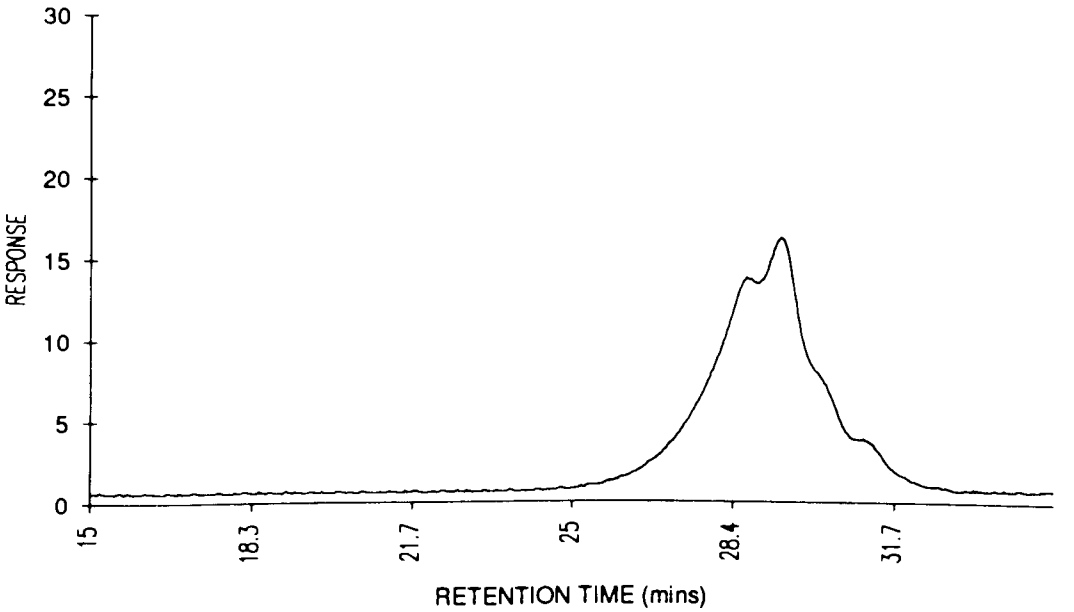

Gel permeation chromatogram of oligomer (**O2**)

FIGURE 9

III.5 Film Formation:

The oligomers formed uniform films when cast from chloroform solution. The films showed patterns of order visible to the naked eye. When placed under a microscope, a definite wave order was observed on the surface of the film. The films were obtained by vacuum deposition or by spin casting. The integrity of the films was good and films could be peeled away from the substrate in methanol regardless of their thickness. This finding contradicts the GPC results which indicates that the molecular weight of the oligomers is below 2000. The order observed in the oligomer films is probably due to the fact that the rigid thiophene segments in the chains are free to align themselves in some semi-crystalline order due to the flexibility of the decane spacers. This behavior might not be restricted to the solid state which would explain the error in the determination of molecular weight by GPC. In fact, if the chains assumed a rigid rod conformation in solution, the GPC molecular weight estimate would be lower than its true value.

III.6 Differential Scanning Calorimetry:

III.6.1 Introduction:

Differential scanning calorimetry (DSC) is the most common technique for analyzing the thermal properties of polymeric materials. It measures energy inputs into a substance and a reference material as they are subjected to a controlled temperature program. The majority of chemical and physical processes involve a change in enthalpy or specific heat which can be detected and quantified by the DSC instrumentation. DSC is used for the determination of heat capacity, heats of transitions, heats of reaction, and temperatures of transition. The technique can also be used in kinetic measurements such as cure rates of resins; rates of thermal, oxidative, and radiative degradation; and rates of physical and chemical changes occurring in polymeric systems[47,48]. The focus of this part of the study was to make preliminary investigations into the thermal characteristics of the oligomers and determine the effect of semi-crystallinity on the morphology of these oligomers. Generally, the convention of the direction of endo - or exo - thermicity has to be indicated since it varies from one instrument to the other. The instrument is usually calibrated by a known standard such as indium metal which has a sharp melting transition. The phase of the resulting melting peak is noted and designated as the direction of endothermicity for the spectra of that instrument. Transitions can manifest themselves in one of two forms:

Second order transitions: an endothermic jump in the heating curve which usually indicates the range of the glass transition temperature (T_g) of the sample. T_g is defined as the temperature at which molecular motion is initiated on a local level in the molecules of the sample. This transition is difficult to observe for polymers since the measurement is complicated by several factors.

At the heating rates employed in DSC (5 - 20 °C/min), the transition occurs slowly, over a temperature range of 10 - 20 °C which may broaden the transition into the baseline. Furthermore, the glassy state is not well defined so that more highly ordered glasses of lower enthalpy and lower glass transition temperatures can be obtained through annealing which can result in a variation in the temperature range and intensity of the transition. As a result, the glass transition temperature is often empirically defined as the temperature at which the tangents to the curve at the initial and final values of the temperature range of the transition intersect[48].

First order transitions: There are three main types of first order transitions which are usually observed by DSC. Melting transitions which are broad endothermic peaks extending over a wide range of temperatures; decomposition transitions which are broad ill - shaped endothermic peaks; and crystallization transitions which are broad exothermic peaks. The broadness of those peaks arises from the presence of polymorphism in most polymeric material which has different transition points. In addition, molecular weight distribution, branching, tacticity, as well as crystallization conditions can affect the intensity and the temperature range of the transitions[48].

A DSC trace can provide information about the thermal and mechanical history of a polymer sample in addition to important thermodynamic and kinetic data. In order to obtain reproducible data, it is of the utmost importance that the samples receive similar thermal treatment since variation in thermal history has a profound effect on thermal characteristics of the samples.

III.6.2 Results and Discussion:

In this work, a positive enthalpic peak corresponds to an endothermic transition, while negative peaks indicate exothermic processes. Figure 10

shows the thermal profile of oligomer (**O2**) film. Films were cast onto sample pans from a chloroform solution to ensure homogeneous thermal exposure. Thermal characteristics were analyzed over a temperature range of 25 °C to 400 °C at the rate of 10 °C/min. The main features of the data are:

A transition at 70 - 80 °C, probably corresponding to the glass transition of the oligomers. The transition is of very low intensity and consequently, is hard to observe. It was found that as the percentage decane spacer increased in the chain, the transition shifted to lower temperature range. In fact, at 1:1 ratio of decane spacer : thiophene, oligomer (**O4**), the transition was observed at 50 - 60 °C.

- A broad first order transition extending over a range of 240 - 290 °C with a maximum at 255 °C was observed for all the oligomers.

- A cooling thermal analysis curve over the same temperature range was featureless as was the subsequent heating curve. The reheating run is shown in Figure 11.

DSC analysis indicates that the oligomers probably go through a glass transition in the range of 50 - 80 °C. Above this temperature the chains are more mobile and can orient themselves to achieve π-stacking of the rigid segments. The effort climaxes by an energy releasing process at the range of 240 - 290 °C. The lack of a melting peak has been attributed to a small latent heat of fusion. Hence the transition is not observable in the DSC scan[49].

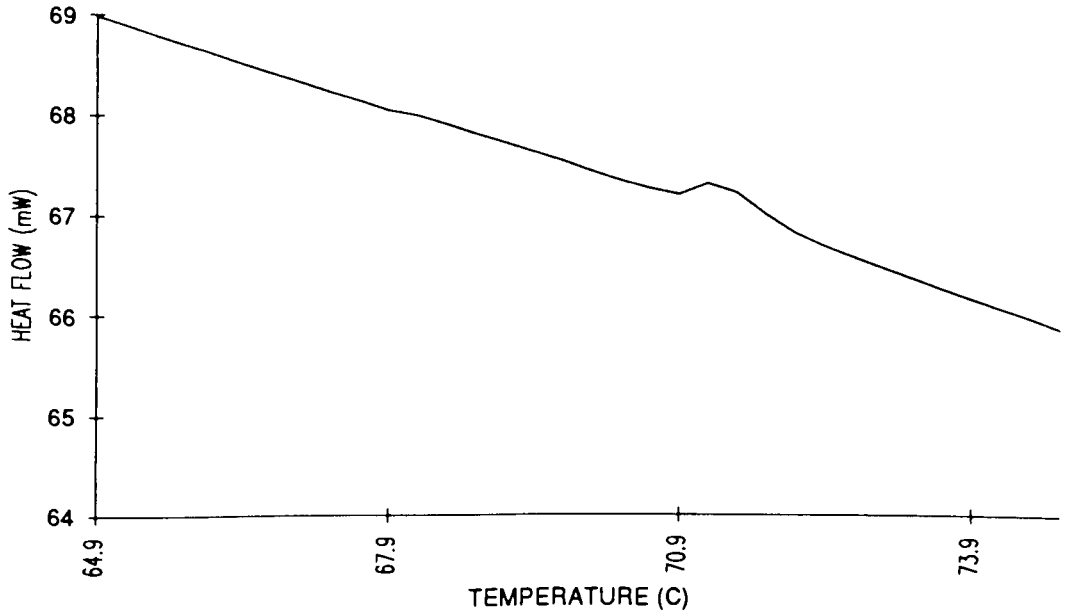

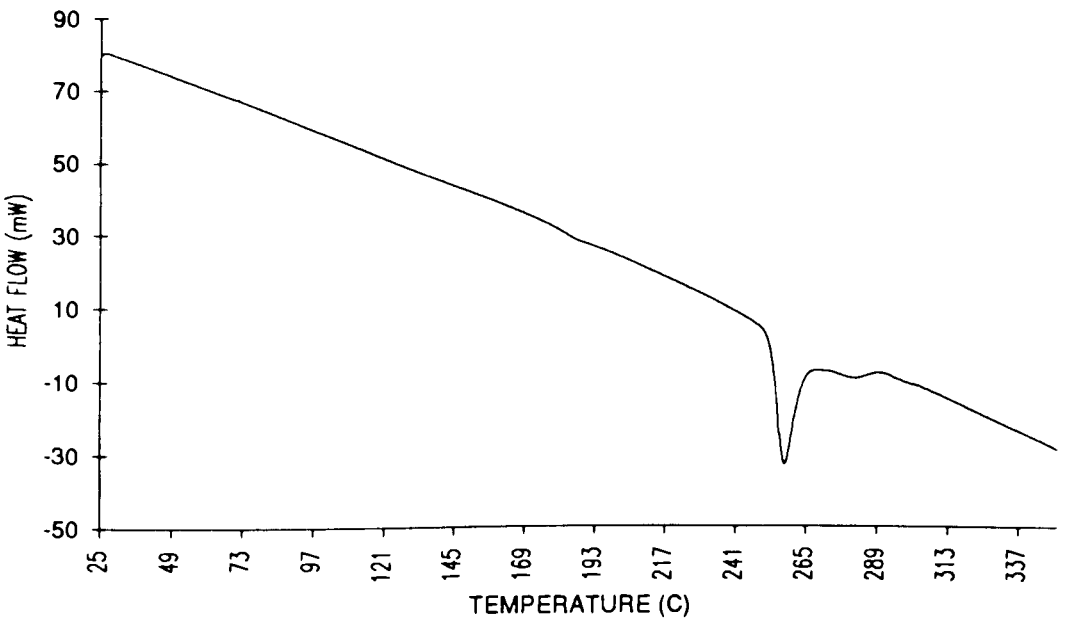

(bottom) DSC thermal profile of oligomer (**O2**) thin film (HEAT).

(top) expanded region

FIGURE 10

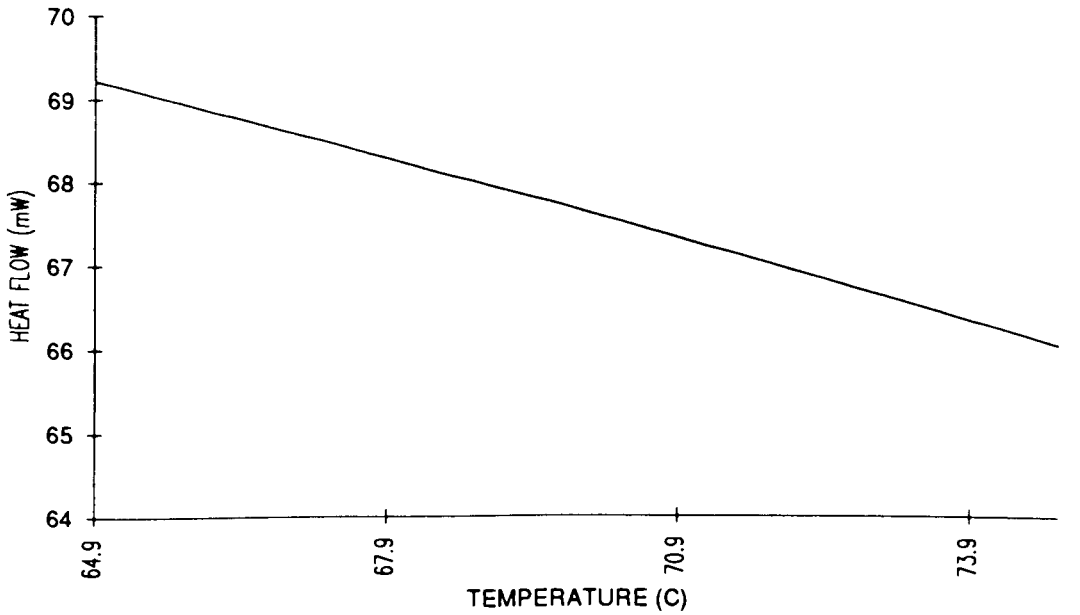

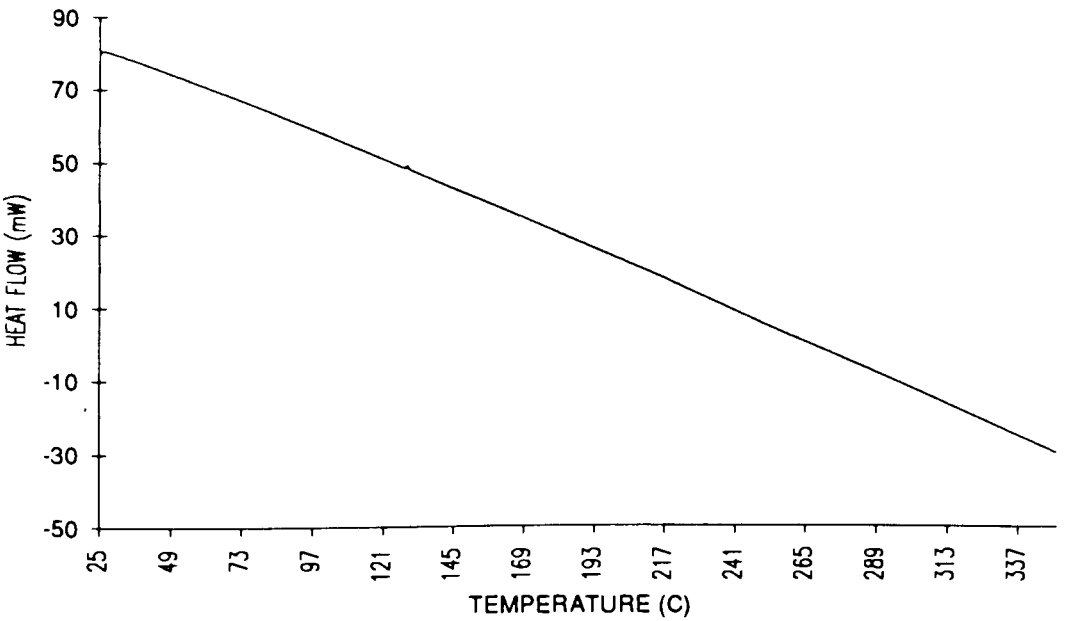

(bottom) DSC thermal profile of oligomer (**O2**) thin film (REHEAT).

(top) expanded region.

FIGURE 11

III.7 Polarization Microscopy Study:

III.7.1 Introduction:

The DSC analysis sparked an interest in the morphology of the oligomer films as a function of temperature. This was investigated further by polarization microscopy. The polarizing microscope is one of the most useful tools used for visually ascertaining the phase of a polymer film at certain conditions. It utilizes the principal of detection and measurement of birefringence[50-53]. Birefringence is defined as the variation of the refractive index of material with respect to direction. A larger refractive index is observed in the direction of greater concentration of polarizable electronic bonds[52]. As linearly polarized light, which is electromagnetic waves oscillating in a single plane, passes through a material, it tends to distort the electronic configuration of the atoms and molecules it encounters. The energy quanta are either absorbed, affecting the transitions in the electronic energy levels of the absorber, or they are merely delayed as they temporarily distort chemical bonds in the medium through which they pass[53]. This latter represents reduced velocity of the light beam as a whole and is expressed as an increase in the refractive index. When polarized light passes through an anisotropic medium, one where molecules are preferentially oriented in a certain direction, the two components of the light vector are slowed to different extents. The component along the optic axis, which is the material's preferred axis of orientation, is delayed less than the component perpendicular to the optic axis[52]. This results in the two components emerging from the material with an optical path difference which can be detected as the phenomenon of birefringence. There are four general types of birefringence[52]:

- Intrinsic birefringence: it results from the inherent asymmetry of polarizability of chemical bonds
- Form birefringence: it originates when objects are regularly oriented within a medium of different refractive index.
- Birefringence of flow: it arises when structures are preferentially oriented in a moving stream of liquid.
- Strain birefringence: it occurs when preferential orientation of structures or realignment of chemical bonds is induced by mechanical stress.

The polarizing microscope is a device in which rotatable polarizers are placed above and below the specimen[50]. The stage can be rotated through 360°, and its orientation measured precisely. Ideally, two polarizing devices in series transmit minimum intensity when their directions of vibration of transmitted beam, azimuth of polarization, are perpendicular. The arrangement is referred to as the cross polarizer position. Alternatively, maximum intensity of transmitted beam is observed when the azimuth of polarization of the two polarizers are parallel. This is referred to as parallel polarizer. In a microscope, the first polarizer is referred to by its name while the second polarizer is given the name analyzer. Between crossed polarizers, an isotropic sample appears dark, while a birefringent sample at the right orientation can transmit a component of modified polarized beam through the analyzer which would result in bright patterns in a dark background being observed[50-53]. The basis of our experiment, was to utilize a hot stage capable of reproducing a uniform increase in the temperature of the sample while monitoring any changes that may occur to the morphology of the sample as it is heated. The analyzer is crossed with the polarizer so that the field of view appears dark. The sample is subjected to the temperature program and the field of view is monitored. If the sample under goes chain movement

which leads to preferential ordering, a birefringence pattern appears indicating deviance from the original morphology of the film. Unfortunately, the hot stage employed could only achieve a maximum temperature of 200 °C.

Oligomer (**O2**) samples were vacuum deposited on thin glass slides. The samples were then placed in the hot stage and monitored while being subjected to a temperature increase of 25 to 200 °C at a rate of 5 °C/min. Micrographs were captured at relevant times using a charge coupled device (CCD).

III.7.2 Results and Discussion:

On the heating cycle, the film homogenized over the surface of the glass slide. However, there was no birefringence observed in the cross polarizer position. As the sample cooled, the film formed small droplets of a diameter of ~ 0.01 - 0.001 μm while maintaining the integrity of the film. Bright yellow patches of a diameter of ~ 0.1 - 1 μm were evident through the cross polarizer, which may point to a nematic phase[54,55]. See Figure 13. Unfortunately, it was not possible to observe the thermal limit of this liquid crystalline phase, nor was it possible to visually determine the precise temperature of transition between the solid and nematic phase. In addition, it was observed that the film cross linked upon continuous exposure to the visible light of the polarizing microscope as shown in Figure 12. The observation was made when the film changed phase except for the area exposed to the light which maintained its initial appearance. This was confirmed by inspecting the birefringence pattern of the film. All areas of the film showed characteristic birefringence except for the exposed area. As a consequence, all other runs were carried out in the dark except when capturing a photograph. As a comparison, a sample of terthiophene was run through the same temperature program. The crystals melted and partially sublimed on to the

cover slide. The pattern of birefringence appeared after cooling and recrystallization of the sample. The pattern was noticeably more defined than that of the oligomers since terthiophene is capable of forming better crystals than the oligomers studied. An objective comparison between terthiophene and segmented oligomers is difficult due to the complication of sublimation. An attempt to run thick oligomer films through the same program resulted in a more homogenous film on the slide, but they were too opaque to transmit any light. A vacuum deposited thin film of poly(3-hexylthiophene) was subjected to the same temperature program as a control experiment. There was no birefringence observed in the temperature range which supports the notion that the observed data is the result of the enhanced flexibility of the oligomers chain and is a characteristic of their unique molecular structure. To understand the potential of these results, a review of liquid crystals is provided[55-59].

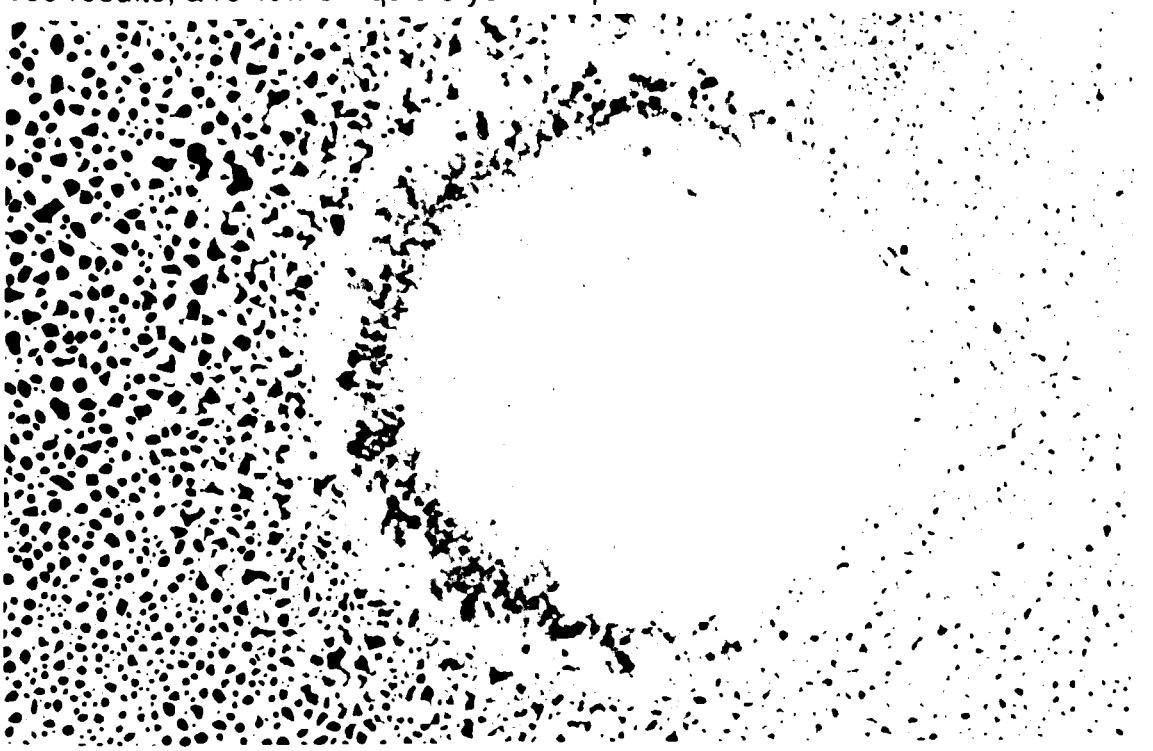

Photograph of the cross linked microscope light exposed area of oligomer (**O2**) thin film

FIGURE 12

(a)

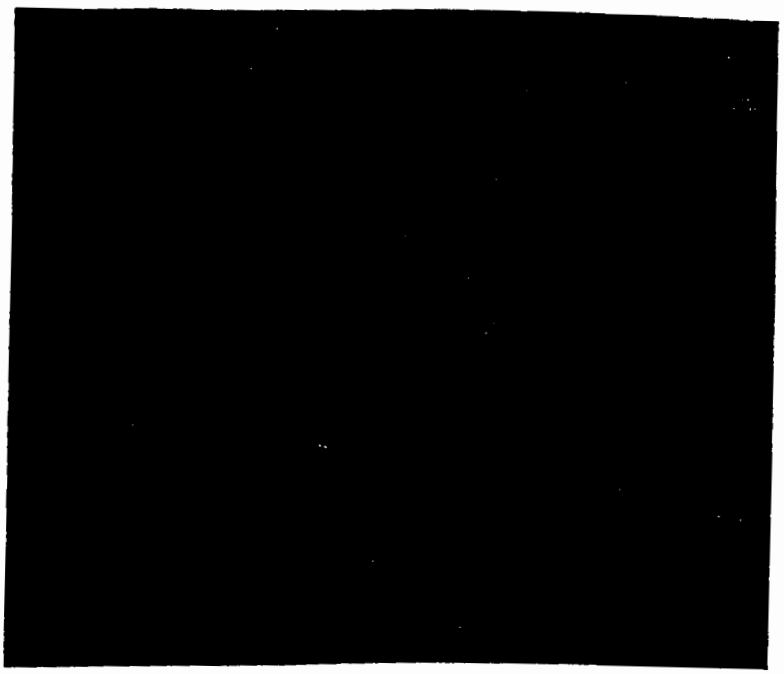

(b)

Birefringence of oligomer (**O2**) thin film; (a) initial, (b) final.

FIGURE 13

III.7.3 Liquid crystallinity:

Liquid crystals are intermediate phase transitions, mesophases, encountered upon passing from a solid to an isotropic liquid. They are classified under two main classes:

* Lyotropic liquid crystals: Mesophases are solvent induced and are highly dependent on the solute concentration. Two examples of this class are DNA and synthetic polypeptides.

* Thermotropic liquid crystals: This class represents the majority of liquid crystals. Transitions are brought about by thermal processes. This class is divided into four subclasses describing the type of order taken on by the liquid crystalline molecule. Refer to figure 14 for an illustration of the subclasses listed below:

~ Smectic order: molecules have long range orientational and translational order. i.e order is lost in only one dimension. There are more than eight characterized smectic phases. Phases S_A and S_C are shown in Figure 14.

~ Nematic order: molecules have long range orientational order but no translational order. i.e, order is present in only one dimension.

~ Cholesteric order: molecules have a nematic order in each plane and the various planes are related via a helical order. In effect, it is chiral nematic order.

~ Discotic order, molecules have long range translational order in two directions and fluidity in the third. This phase is similar to smectic order. However, the molecules are disc-shaped in contrast to rods in the regular smectic phases

For any of the above orders to exist, there are two main features that have to be characteristic of the molecule in question. These are: asymmetry of the molecular shape, and anisotropy of intermolecular forces. As far as polymers are concerned, the majority of polymers consist of long highly asymmetrical molecules that prefer a certain orientation. These molecules should favor the formation of liquid crystalline states. It is found that the flexibility of the backbone of the main chain liquid crystalline polymers is instrumental in the stabilization of the mesophases. Flexible chain polymers such as polyethylene tend to form random coils which lower the size of the regions of spontaneously ordered segments of the macromolecules. These regions are usually too small for the manifestation of anisotropy of properties by the polymeric material. Liquid crystallinity can also be induced by the application of mechanical force, electrical, or magnetic external fields. Polymers which fall in this category are usually referred to as viscocrystalline as opposed to liquid crystalline. Rigid chain polymers such as aromatic polyesters thermodynamically favor a conformation that maximizes order among the chains or segments thereof. This may lead one to believe that all rigid chain polymers exhibit liquid crystalline states, but this is untrue. It is quite difficult to predict if a polymer will exhibit liquid crystalline transitions. However, one can predict if a polymer is a candidate to form liquid crystalline state with reasonable accuracy. Polythiophenes appear to have the requirement for forming mesomorphic states.

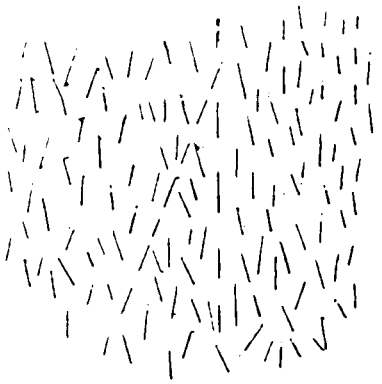

(a) nematic order

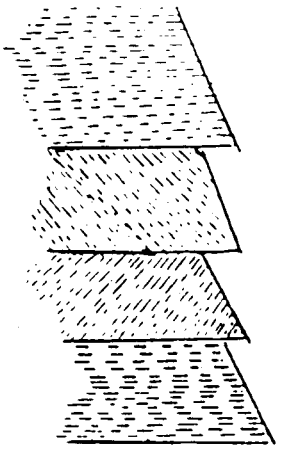

(b) cholesteric order

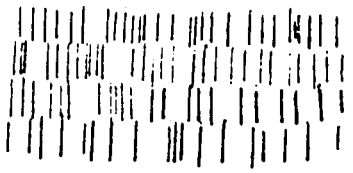

(c) smectic A (S_A) order

(d) smectic C (S_C) order

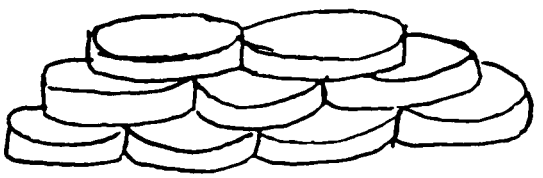

(e) discotic order

Illustration of subclasses of thermotropic liquid crystals

FIGURE 14

They do possess micro crystalline regions. However, no liquid crystalline behavior has been reported to date. This could be attributed to their slow relaxation process. In other words, the polymer melts or decomposes upon heating before the chains are able to arrange into partial order. However, it was found that α - sexithienyl formed a nematic phase at high temperatures[54]. A crystal to mesophase transition was observed at 312 °C. No isotropic melting transition was observed which was attributed to the small latent heat of fusion[49]. This finding reinforces the validity of the phase interpretation made for the oligomers prepared in this study since they are essentially made up of small oligothiophenes interlinked with flexible decane spacers.

III.8 Electronic conductivity Study:

III.8.1 Introduction:

Conductivity (σ) is defined as the reciprocal of the resistivity (ρ) to current flow through a material. Good conductors are materials with low resistivity while the opposite is true for semiconductors and insulators. Conductivity is dependent on factors such as temperature, geometrical dimensions, the type of the conduction mechanism, and the nature of charge carriers[60]. In order to minimize errors in resistivity measurements, a collinear four probe technique was used under isothermal conditions. This technique is recommended for resistivity measurements of samples with a variety of shapes and irregular boundaries[60]. It is also used for samples with regions of varying resistivity. The technique utilizes four pointed equispaced probes in contact with the plane surface of the sample. A uniform film is made in order to minimize the variance of resistivity in the sample. Current is passed through the two outer probes while the potential difference is measured across the two inner probes[60]. The voltage measured is used in the calculation of the material's resistivity by equation 1.

$$\rho = (V / I) ((\pi d) / \ln 2) \qquad \text{equation 1}$$

where

ρ is the resistivity of the oligomer film.

V is the potential difference between the inner two probes.

I is the current passed through the outer two probes.

d is the thickness of the film.

Equation - 1 - holds with the assumption that the thickness of the film (d) << the distance between two probes. The conductivity of the film is obtained by taking the reciprocal of the calculated resistivity as shown in equation 2.

$$\sigma = 1 / \rho \qquad \text{equation 2}$$

Constraints associated with the method include[60]:

- The probes must be far removed from any sample boundary.
- The diameter of the contact of each probe and the sample surface must be small in comparison to the inter probe distance.
- The sample surface must have a high electron recombination rate to minimize the effect of probe injected electron or holes.
- The boundary between the current carrying probes and the sample must be small in diameter and hemispherical in shape.

III.8.2 Results and Discussion:

A thin film (~ 0.5 - 1 μm) of oligomer (**O2**) was spin cast from a 20 mg/ml chloroform solution. The uniform film was dipped for 5 seconds in a 0.1 M solution of ferric chloride in nitromethane. The color of the film changed upon oxidation from dark red to deep blue. The film was immersed in nitromethane for 5 - 10 second to remove excess ferric chloride. Using the collinear four probe technique, the conductivity of the oxidized thin film was determined to be in the range of 10^{-3} to 10^{-4} S / cm. The result is in agreement with the expected reduction of the conductivity upon disruption of the interchain conduction mechanism. The oxidized film was found to be stable for one month in the dark at ambient conditions. The small magnitude of the conductivity of the material prevented the monitoring of the stability of the oxidized film by its conductivity.

However, the absorption spectrum, shown in figure 15, showed a decrease in the π to π^* absorption in favor of the appearance of a bipolaron absorption centered at 644 nm and extending to 800 nm. The shape of the new absorption band is in accordance with the fact that the material has various lengths of conjugated thiophene segments. The bipolaron absorption is similar to that of poly(3-hexylthiopene) with the latter's absorption maximum being at 750 nm. The bipolaron absorption decreased with time and the color of the film faded to a minimum after a period of one month as reported above.

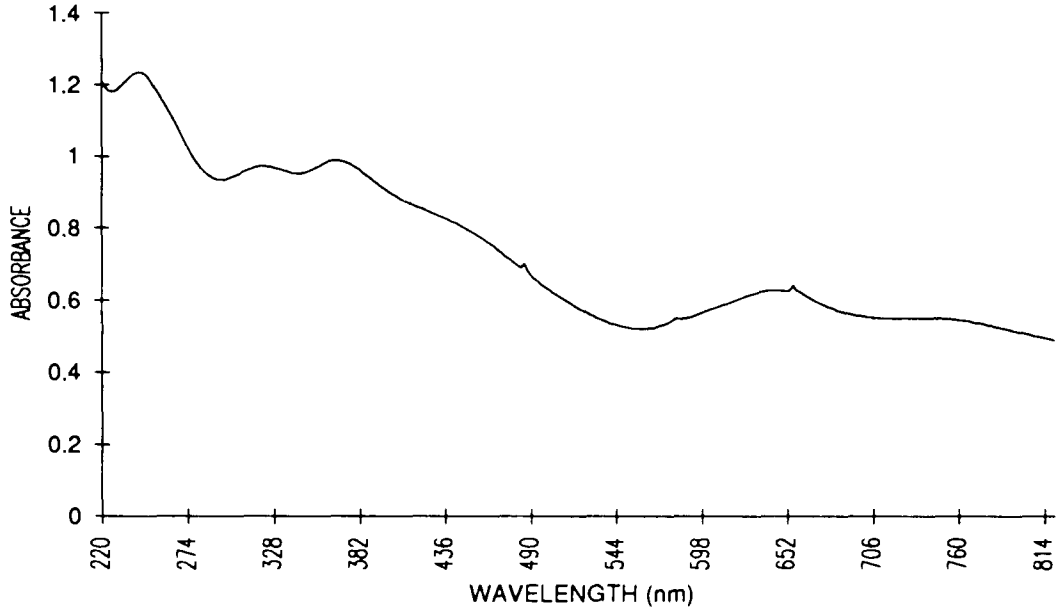

UV-vis absorption spectrum oxidized oligomer (**O2**) thin film

FIGURE 15

CHAPTER IV CONCLUSIONS:

The feasibility of interconnecting short rigid thiophene segments with flexible spacers was investigated and the properties of the resulting oligomers were compared to poly(3-hexylthiophene). The oligomers were synthesized by the copolymerization of 2,5-diiodothiophene with 1,10-di((5-iodo)-2-thienyl)decane via the Grignard method. The chemical yield and molecular size of the products were found to be a function of the susceptibility of the number 5 thiophene carbon in 1,10-di((5-iodo)-2-thienyl)decane to nucleophilic attack. Four oligomers were synthesized. The chemical structure of the oligomers was confirmed by ^1H NMR spectroscopy, and the ratio of decane spacer : thiophene units in the oligomer molecules was determined (chapter III.3). Their decane spacer content ranged from 18 - 50 mol% (chapter II).

These oligomers are much less soluble than poly(3-hexylthiophene). This was attributed to the inability of the decane spacers to affect the intermolecular distance of the thiophene segments to the same extent as a substituent at the 3 - position of the thienyl ring in the case of poly(3-hexylthiophene). This indicated a higher degree of molecular order for the oligomers.

The UV-vis spectroscopy of tetrahydrofuran solutions of the oligomers indicated that their average conjugation length decreased as the molar ratio of decane spacer : thiophene was increased. However, the average number of thienyls per thiophene segment could not be precisely determined. The solid state absorption spectrum of a thin film of oligomer (**O2**) was similar to that of its solution. This is in contrast to poly(3-hexylthiophene) which exhibits a red shift on going from solution to solid state presumably because the average π-conjugation length increases. The similarity between the solid state and solution

spectra of the oligomers led to the deduction that the oligomer molecule possesses a similar conformation in solid state and in solution (chapter III.2).

In an attempt to determine the molecular weight of these oligomers, gel permeation chromatography (GPC) was utilized. Absolute molecular weights could not be obtained due to the uncertainty in the calibration of the GPC. The molecular weights determined were used as a relative measure to compare the oligomers. These molecular weight values were low and within the same order of magnitude (chapter III.4), and consistent with the limitation of chain growth described in chapter II.

In spite of their apparent low molecular weight, the oligomers formed uniform thin films that showed a definite order under the microscope. Furthermore, films could be peeled away from the glass substrate in methanol to yield free-standing films of sub-micron thickness (chapter III.5).

Thin films of oligomer (**O2**) were investigated further using a hot-stage polarization microscope. The films cross linked upon prolonged exposure to the microscope light. This necessitated that microscopy experiments had to be carried out in the dark except when capturing a photograph. On the heating cycle, films homogenized into a more uniform surface morphology and small droplets of a diameter of ~0.01 - 0.001 μm were visible at a magnification of 5x. These droplets were suspected of being evidence for the existence of a nematic liquid crystalline phase. No thermal transitions supporting this supposition were observed in the DSC investigation of these oligomers (chapter III.6). In addition, the films failed to show birefringence during the heating cycle when observed through cross polarizers. However, upon cooling to room temperature, bright yellow batches with a diameter of ~ 0.1 - 1 μm were evident through the cross polarizers (chapter III.7). This indicated a change in the molecular ordering of the films. These transitions were not observed for a similarly treated poly(3-

hexylthiophene) films. The birefringent regions of the films are probably due to highly ordered thiophene segments. This may be clarified by X-ray diffraction studies.

Electronic conductivity is one of the most important properties of poly(3-hexylthiophene). Therefore, the effect of the oligomer's novel structure on the electronic conductivity of the thienyls was of interest. Films of the oligomers oxidized in nitromethane solutions of ferric chloride. Upon oxidation, the films changed color from red to blue. Oxidation was confirmed by the absorption spectra of the films which showed a decrease in the $\pi \rightarrow \pi^*$ transition optical density and the growth of a new broad band at 644 nm and having an absorption tail which extended over beyond 800 nm. The conductivity was 10^{-3}-10^{-4} S/cm (chapter III.8). Since the intramolecular mechanism was eliminated by virtue of the structure of the oligomers, charge carriers conduction is sustained via an intermolecular conduction mechanism (chapter I).

In closing, more research is required to fully investigate the properties of these oligomers. Nevertheless, this work has succeeded in demonstrating the feasibility of obtaining novel π-conjugated oligomers and illustrated some of the interesting properties associated with them.

REFERENCES

1. Chiang, C. K.; Fincher, C. R.; Park, Y. W.; Heeger, A. J.; Shirakawa, H.; Louis, E. J.; Gau, S. C.; and McDiarmid, A. G. *Phys. Rev. Lett.* **1977**, 39, 1098.

2. Overview of conducting polymers in; (a) Proceedings of the international conference on conducting polymers. *J. Phys. (les ulis fr.).* **1983**, 44, C3; (b) Proceedings of the work shop on synthetic metals. *Synth. Met.* **1984**, 9, 129; (c) Proceedings of the international conference on synthetic metals. *Mol. Cryst. Liq. Cryst.* **1985**, 117-121; (d) Skotheim, T. J.,Ed., Dekker, M. ' " *Hand Book on Conducting Polymers*". Newyork.; (e) Gill, W. D.; Clarke, T. C.; Street, G. B. *Appl. Phys. Commum.* **1982**, 2, 211.

3. Roncali, J. *Chem. Rev.* **1992**. 92, 711.

4. Baker, G. L. "*Electronic and Photonic Applications of Polymers*"; Bowden, M. J.; Turner, S. R. Eds.; *ACS Advances in Chemistry Series 210; American Chemical Society.* Wash, D. C. **1988**. P 271.

5. Bredas, J. L.; Street, G. B. *Acc. Chem. Res.* **1985**, 18, 309.

6. Diaz, A. F. *Chem. Ser.* **1981**, 17, 142.

7. Tourillon, G.; Garnier, F. *J. Electroanal. Chem.* **1982**, 135, 173.

8. Bargon, J.; Mohamand, S.; Waltman, R. J. *IBM. J. Res. Develop.* **1983**, 27, 330.

9. Delamar, M.; Lacaze, P. C.; Dumousseau, J. Y.; Dubios, J. E. *Electrochim, Acta.* **1982**, 27, 61.

10. Roncali, J.; Garreau, R.; Yassar, A.; Marque, P.; Garnier, F.; Lemaire, M. *J Phys. Chem.* **1987**, 91, 6706.

11. Sugimoto, R.; Takeda, S.; Gu, H. B.; Yoshino, K. *Chem Express.* **1986**, 1, 635.

12. Hotta, S.; Soga, M.; Sonoda, N. *Synth. Met.* **1988**, 24, 223.

13. Yoshino, K.; Nakajima, S.; Onoda, M.; Sugimoto, R. *Synth. Met.* **1989**, 28, C349.

14. Lin, J. M. P.; Dudek, L. P. *J. Polym.Sci.* **1980**, 18, 2869.

15. Yamamoto, T.; Sanchika, K.; Yamamoto, A. *Bull. Chem. Soc. Jpn.* **1983**, 56, 1503.

16. Tamao, K.; Kumada, M.; Kodama, S.; Nakajima, I.; Minato, A.; Suzuki, K. *Tetrahedron.* **1982**, 38, 3347.

17. Holdcroft, S.; Mao, H. *Macromolecules.* **1992**, 25, 554.

18. Winokur, W. J.; Spiegel, D.; Kim, Y.; Hotta, S; Heeger, A. J. *Synth. Met.* **1989**, 28, C419.

19. Gallazzi, M. C.; Castellani, L.; Zerbi, G.; Sozzani, P. *Synth. Met.* **1991**, 41 -43, 495.

20. Mandalen,J.; Somuelsen, E.; Gautun, O. R.; Carlsen,P. H. *Solidstate. Commen.* **1991**, 77, 337.

21. Cui, C. X.; Kertesz, M. *Phys. Rev. B.* **1989**, 40, 9661.

22. Roncali, J.: Lemaire, M.; Garreau, R.; Garnier, F. *New. J. Chem.* **1987**, 11, 703.

23. Galvao, G. S.; Dos Santos, D. A.; Laks, B.; Dos Santos, M. C. *Synth. Met.* **1991**, 41-43, 3521.

24. Wudl, F.; Souto-Maior, R. M. *Synth. Met.* **1989**, 28, C281.

25. Wudl, F.; Souto-Maior, R. M.; Hunkelmann, K.; Eckert, H. *Synth. Met.* **1990**, 23, 1268.

26. Holdcroft, S; Xu, B, *Macromolecules.* **1993**, 26, 4457.

27. Nechtschien, M.; Derreux, F.; Genoud, F.; Vieil, E.; Pernaut, J. M.; Genies, E. *Synth. Met* **1986**, 15, 59.

28. Kaneto, K.; Yoshino, K.; Inuishi, Y. *Jap. J. App. Phys.* **1986**, 21, 147.

29. Bredas, J. L.; Themans, B.; Andre, J. M.; Chance, R. R.; Silbey, R. *Synth. Met.* **1984**, 9, 265.

30. Ito, M.; Shiode, H.; Tanaka, K. *J. Polymer. Sci.* **1986**, 24, 147.

31. Tanaka, S.; Kutz, H. E.; Hutton, R. S.; Overstein, J.; Fredrickson, G. H.; Wong, T. T. *Synth. Met.* **1986**, 16, 17.

32. Sato, M.; Tanaka, S.; Kaeriyama, K. *J. Chem. Soc., Chem. Comm.* **1986**, 873.

33. Lemaire, M.; Roncali, J.; Garnier, F.; Garreau, R.; Hannecant, E. H. *French. Pat.* 86.04744,**april 4,1986**.

34. Hotta, S.; Rughooputh, D. D. V.; Heeger, A. J.; Wudl, F. *Macromolecules.* **1987**, 20, 212.

35. Osterholm, J. F.; Luakso, J.; Nyholm, P.; Isotato, H.; Stubb, H.; Inganas, O.; Salaneck, W. R. *Synth. Met.* **1989**, 28, C435.

36. Kobayashi, M.; Chen, J.; Chung, T. C.; Moraes, F.; Heeger, A. J.; Wudl, F. *Synth. met.* **1984**, 9, 77.

37. Monteheard, J. P.; Pascal, J.; Seytre, G.; Stettam-Boiteau, G.; Donillard, H. *Synth. Met.* **1984**, 9, 389.

38. Ruiz, J. P.; Gielselman, M. B.; Nayak, K.; Marynick, D. S.; Reynolds, J. R. *Synth. Met.* **1989**, 28, C481.

39. Nillsson, J. O.; Gastafsson, G.; Inganas, O.; Uvdal, K.; Salaneck, W. R.; Laaks, J.; Osterholm, J.E. *Synth. Met.* **1989**, 28, C445.

40. McCullough, R. D.; Lowe, R. D. *J. Chem. Soc., Chem. Comm.* **1992**, 70.

41. Pham, C. V.; Burkhault, A.; Shabana, R.; Cunningham, D. D.; Mark, , Jr, H. B.; Zimmer, H. *Phosphorus, Sulfur, and Silicon.* **1989**, 46, 153.

42. Shabana, R.; Galal, A.; Mark, Jr, H. B.; Zimmer, H.; Gronowitz, S.; Hornfeidt, A. B. *Phosphorus, Sulfur, and Silicon.* **1990**, 48, 239.

43. Curtis, R. F.; Phillips, G. T. *Tetrahedron.* **1967**, 23, 4419.

44. Miraw, P. A. " *Polymer Characterization*". Hunt, B. J.; James, M. I. Eds. Blackie Academic & Professional. **1993**, P 37-68

45. Tonelli, A. E. "*NMR Spectroscopy and Polymer Microstructure, The Conformational connection.*" VCH Publishers ,*Inc.* **1989**.

46. Wetton, R. E. "*Polymer Characterization*". Hunt, B. J.; James, M. I. Eds. Blackie Academic & Professional. **1993**, P 178-220.

47. Allcock, H. R.; Lampe, F. W. "*Contemporary Polymer Chemistry*". 2nd Ed. Prentice hall, Inc. **1990**.

48. *Encyclopedia of Polymer Science and Engneering.* Suppl Vol. John Wiley & sons, Inc. **1989**, P 711.

49. Detsri, S.; Mascherpa, M.; Porzio, W. *Adv. Mater.* **1993**, 5, No.1, 43-45.

50. Vaughan, A. S. "*Polymer Characterization*". Hunt, B. J.; James, M. I. Eds. Blackie Academic & Professional. **1993**, P 297-306.

51. Rochow, T. G.; Rochow, E. G. "*An Introduction To Microscopy By Means Of Light, Electrons, X rays, Or Ultrasound*".Plenum Press, Newyork. N. Y. **1978**.

52. Spencer, M. "*Fundamentals Of Light Microscopy*". Cambridge University Press. **1982**.

53. Slayter, E. M.; Slayter, H. S. "*Light And Electron Microscopy*". Cambridge University Press. **1992**.

54. Taliani, C.; Zamboni, R.; Rnani, G.; Rossini,S.; Lazzaroni, R. *J. Mol. Electron.* **1990**, 6, 225.

55. Noel, C. "*Recent Advances In Liquid Crystalline Polymers*". Elsevier Applied Science Publishers LTD. **1985**, P 135-165.

56. Priestley, E. B. "*Introduction To Liquid Crystals*". Plenum Press. Newyork, N. Y. **1975**, P 1-12.

57. Bahadur, B. "*Liquid Crystals , Applications And Uses*". World Scientific Publishing Co. LTD. **1990**.

58. Plate, N. A.; Shibaer, V. P. "*Comb-Shaped Polymers And Liquid Crystals*". Plenum Press. Newyork, N. Y. **1987**.

59. Sirign, A. "*Liquid Crystallinity In Polymers*".VCH Publishers, Inc. **1991**, 261 -315.

60. Wieder, H. H. "*Laboratory Notes On Electrical And Galvanomagnetic Measurements*". Elsevier Scientific Publishing Company. **1979**.